2002

Adhesive bonding of a novel liquid crystal thermoset

Benjamin Allen Dietsch
University of Dayton

ADHESIVE BONDING OF A NOVEL LIQUID CRYSTAL THERMOSET

THESIS

Submitted In Partial Fulfillment of the Requirements for The Degree
Master of Science in Chemical Engineering

By
Benjamin Allen Dietsch

Graduate Research and Engineering
School of Engineering
UNIVERSITY OF DAYTON
Dayton, Ohio
April, 2002

ADHESIVE BONDING OF A NOVEL LIQUID CRYSTAL THERMOSET

APPROVED BY:

[redacted]

Richard P. Chartoff, Ph.D.
Advisory Committee Chairman
Co-Research Advisor
Professor, Chemical and Materials Engineering

[redacted]

Donald A. Klosterman, Ph.D.
Committee Member
Co-Research Advisor
Professor, Chemical and Materials Engineering

[redacted]

Kevin J. Myers, D.Sc., P.E.
Committee Member
Academic Advisor
Professor, Chemical and Materials Engineering

[redacted]

Patrick J. Hood, Ph.D.
Committee Member
President and Chief Scientist
Cornerstone Research Group, Inc.

[redacted]

Donald L. Moon, Ph.D.
Associate Dean
Graduate Engineering Programs and Research, School of Engineering

[redacted]

Blake E. Cherrington, Ph.D., P.E.
Dean, School of Engineering

ABSTRACT

ADHESIVE BONDING OF A NOVEL LIQUID CRYSTAL THERMOSET

Name: Dietsch, Benjamin Allen
University of Dayton, 2002

Research Advisors: Dr. R.P. Chartoff and Dr. D.A. Klosterman

The goal of this work was to examine the adhesion of a novel liquid crystal (LC) thermoset, JNM-1, to aluminum. More specifically, the effects of LC resin cure state and morphology and aluminum substrate surface treatment on tensile lap shear strength were determined. The cure state of the thermoset relates to the crosslink density and the morphology relates to the LC domain structure. Both of these have an effect on the strength and toughness properties of the thermoset. Cure cycles were developed to cure the monomer in the isotropic and LC phase using Differential Scanning Calorimetry and polarized optical microscopy. These cure cycles were used to cure the adhesive on lap shear coupons for testing. The lap shear results show that there is no substantial effect of these cure cycles on lap shear strength.

Overall analysis of the bonding process in this work shows that cohesive failure is necessary to reveal the strength of the adhesive. The use of PAA treatment on aluminum is critical to determine the cohesive strength of the bond between aluminum and JNM-1. The highest average lap shear strength for JNM-1 on 2024-T3 aluminum was 1835 psi. This value corresponds to JNM-1 cured in the LC state on adherends treated with PAA and primed with BR-127 epoxy phenolic

primer. Due to the large number of samples used in this study, a modified fabrication method was used to prepare lap shear coupons in a timely manner. Lap shear strengths from coupons prepared using the modified method yielded similar trends when compared to coupons prepared using the ASTM standard method.

ACKNOWLEDGEMENTS

I would like to thank the people of the Center for Basic and Applied Polymer Research and the people of Cornerstone Research Group, Inc. for providing this opportunity to me. Specifically, I would like to thank Dr. Richard Chartoff and Dr. Don Klosterman for their guidance in all phases of this project, especially fundamental issues regarding the adhesion process, polymer mechanics, and the importance of patience and perseverance. I would like to thank Dr. Tat Tong for guidance in the chemical aspects of the project and for conversations about the importance of humanity. I would like to thank Mary Galaska and Bobby Russell for technical help with laboratory work, for good laughs, and for teaching me how to speak Texan. I would like to thank John Stalter and Gary Andrews for help in aluminum treatment and for letting me bug them at any time. I would like to thank Dr. Patrick Hood for his overall support of the project and for asking me what I wanted out of it all. And I would like to thank Chrysa Theodore for her technical advice and for her support in making this project a great experience for me, both professionally and personally.

I would also like to thank my mom and dad, Sandy and Roger Dietsch, and my friend Ashley Schoulties for their moral support and "big picture" attitude throughout the entire research process. Their support, and the effects of playing rugby, helped me through many times of frustration.

Finally, I would like to thank the Air Force Office of Scientific Research (AFOSR) who provided the funding for the initial aspects of this project through the Phase II STTR contract # F49620-99-C-0037 titled "High Performance Liquid Crystal Adhesives" and Cornerstone Research Group, Inc. for providing the funding to finish the work. I would also like to thank the Dayton Area Graduate Studies Institute for providing financial support for tuition.

TABLE OF CONTENTS

ABSTRACT.....iii
ACKNOWLEDGEMENTS.....v
TABLE OF CONTENTS.....vi
LIST OF FIGURES.....viii
LIST OF TABLES.....ix
CHAPTER I: INTRODUCTION.....1
1.1 Rationale for the Research Program.....1
1.2 Program Objectives.....3
1.3 Background.....3
1.3.1 Liquid Crystal Thermosets.....3
1.3.2 Importance of the Bond Interface.....6
1.3.3 Substrate Surface Preparation.....7
CHAPTER II: EXPERIMENTAL PROCEDURE.....11
2.1 Experimental Overview.....11
2.2 Development of Adhesive Cure Cycles.....11
2.3 Development of Surface Preparation Techniques.....14
2.4 Silane Application Process – Dissolution method.....17
2.5 Lap Shear Coupon Fabrication and Testing.....19
CHAPTER III: RESULTS AND DISCUSSION.....22
3.1 Cure Cycle Development and Analysis.....22
3.2 Dissolution Method Results.....24
3.3 Lap Shear Testing Results.....26
3.3.1 Effect of Failure Mode on Lap Shear Strength.....26
3.3.2 Effect of Silane Treatment and Cure Cycle on Lap Shear Strength.....31

3.3.3 Effect of Sample Fabrication Method on Lap Shear Strength.....33
3.3.4 Comparison of JNM-1 Lap Shear Strength to Conventional Aerospace Adhesives.....35
CHAPTER IV: CONCLUSIONS.....36
REFERENCES.....38

LIST OF FIGURES

1. JNM-1 liquid crystal monomer structure.....5
2. DSC thermograms illustrating the effect of 1% benzoyl peroxide (BP) initator in shifting the main cure reaction to a lower temperature. Heating rate = 5°C/min; argon atmosphere.....13
3. Chemical Structures of Silane Coupling Agents.....16
4. Comparison of Tabs Used For the Dissolution Method.....19
5. Custom Jig Used for Lap Shear Coupon Fabrication.....21
6. Cure cycles selected for JNM-1 in the a) isotropic and b) LC phase.....22
7. DSC thermograms illustrating the progress of cure for JNM-1 with 1% benzoyl peroxide (BP); The upper curve is for an uncured sample, while the other curves are for samples cured following the two cure paths illustrated in Figure 6.....23
8. Polarized optical photomicrograph of a thin film of JNM-1 with 1% BP, cured in the LC phase (100X).....25
9. Lap shear coupons; the top coupon exhibits adhesive failure while the bottom coupon exhibits cohesive failure.....27
10. Variations in scrim and adhesive patterns for samples showing cohesive failure.....28
11. Comparison of initial surface treatment to average lap shear strength 29
12. Stereo micrograph (a) and isometric illustration (b) of the oxide layer of PAA treated aluminum [39].....30
13. Comparison of surface treatment and cure conditions to average lap shear strength 32
14. Comparison of fabrication method to average lap shear strength.....34

LIST OF TABLES

1. Test matrix for surface preparation variables.....14

CHAPTER I

INTRODUCTION

1.1 Rationale for the Research Program

The use of adhesives in place of mechanical fasteners in the aerospace industry has revolutionized the fields of aircraft construction and repair. An adhesive bond at a joint distributes the joint stresses across the entire bondline, whereas a mechanically fastened joint produces stress gradients between fastened and unfastened areas. The result of an even stress distribution across a bondline is improved joint efficiency. This reduces the amount of material needed for fabrication or repair and allows for the fabrication of joints in places where it would have been difficult using mechanical methods. Also, adhesively bonded joints are mechanically less susceptible to corrosion due to the lack of fastener holes throughout the bondline, thereby increasing the life of the joint. The use of adhesives is also crucial when dealing with composite structures. Many composite materials lose considerable strength when mechanically altered, due to their anisotropic nature, and require adhesive bonding when used in such structures. The major drawbacks of adhesives for bonding are the processing and environmental limitations of the adhesive material.

Most aerospace adhesives are thermosetting polymers, which have an upper use temperature typically lower than that of aluminum, steel, or titanium. Also, adhesive bonds usually require careful surface preparation of the adherend surfaces in order to obtain optimal bond performance. Most adhesives are cured thermally and under pressure, which requires the use of equipment larger than the bondline. This makes the bonding of major aircraft structures difficult. In comparison, mechanical fastening is easier to perform and may be a faster process in some situations. However, adhesives are

robust materials despite their inherent disadvantages, and there exists a huge industry dedicated to the development of new materials for use as aerospace adhesives.

A major goal in the aerospace adhesives industry is to research and develop materials that give high bond strengths within a broad range of environmental conditions. Also, these materials should be easy to process and function on a variety of substrates. Unfortunately, one material does not exist that fulfills all of these requirements. There are, however, polymeric materials that are sufficiently robust to fulfill most of these requirements. For example, epoxy-based thermosets have demonstrated high strength and endurance properties on aluminum and composite substrates and have been used for several decades as structural aerospace adhesives [1]. Early epoxy thermosets were criticized for low toughness properties, but current epoxy formulations possess increased toughening mechanisms in the form of small, embedded elastomeric particles. The upper use temperatures for most epoxies range from 150-200°C. Polyimide-based thermosets are also used as aerospace adhesives. These materials generally possess high strengths at temperatures up to 300°C, after a thermal cure at or above this temperature [2]. However, processing of these resins is more difficult and the cured material tends to be very brittle. More recently, liquid crystal thermosets have been proposed as candidates for adhesives applications because of their superior mechanical properties and high upper use temperatures. The superior properties of these materials are related to their molecular structure and state of cure and include increased toughness, high temperature stability, and good hygrothermal (high humidity, high temperature) resistance.

A key issue in researching and developing an adhesive for aerospace structures is the use of proper surface preparation when fabricating test components. The molecular interactions between adhesive and adherend are equally as important to the integrity of the bond as the molecular interactions within the adhesive. Different surface preparations are used for different surfaces and with different adhesives. Research into the effects of surface preparation on adhesion is focused on the chemical and physical mechanisms behind the interaction between adhesive and adherend. Although these exact mechanisms are not known in some cases, standard surface preparation procedures exist

for common substrates and are widely used throughout the adhesive industry and in research into new adhesives.

1.2 Program Objectives

The major goal of this work is to examine the adhesion of a novel liquid crystal (LC) thermoset to aluminum. More specifically, the effects of LC resin cure state and morphology and aluminum substrate surface treatment on tensile lap shear strength will be determined. The cure state of the thermoset relates to the crosslink density and the morphology relates to the LC domain structure. Both of these may have an effect on the strength and toughness properties of the thermoset. Appropriate cure cycles will be determined from thermal and microscopic analysis of the liquid crystal thermoset. The effects of cure state and morphology will be investigated in parallel with the effects of adherend surface treatment. The type of surface treatment for aluminum substrates used in lap shear testing has a direct effect on the physical and chemical interactions between the liquid crystal thermoset and the aluminum adherend. Standard aluminum surface treatments will be used to determine these effects. The combined influence of cure state and morphology, along with surface treatment will be used to evaluate the effectiveness of the adhesive in comparison to other standard adhesives. Initial aspects of this work were presented in a previous paper [3].

1.3 Background

1.3.1 Liquid Crystal Thermosets

The function of an adhesive is accomplished when force from one substrate is transmitted through the adhesive-adherend interface, into and through the adhesive network, and through the opposing interface into the other substrate. Strength within the adhesive bulk is crucial to the strength of the bond as long as forces are effectively transmitted through the interfaces. The strength of the adhesive is determined by the polymer molecular network, which is a function of material properties and cure

conditions. Also, the micro-morphology of the polymer network can affect the strength of the adhesive. As discussed previously, many conventional aerospace adhesives are polymeric thermoset materials, such as epoxies and polyimides, with well-known characteristics and limitations. The use of liquid crystal monomers to form a resin network for adhesion is an attempt to overcome some of these limitations. In order to understand the rationale behind this, it is necessary to understand the properties of liquid crystalline materials in general.

Liquid crystalline materials were observed as early as 1888, when it was shown that certain cholesteryl esters changed from colored and opaque to clear when heated [7]. This change signified a molecular rearrangement within the material, which was later identified as a transition, or mesomorphic, phase between the crystalline solid phase and the isotropic melt phase [8]. This ordered transition phase is best understood when examined at the molecular level. A liquid crystal (LC) monomer is characterized by a rigid rod core capped by flexible "spacer" end groups. The rigid rod core is usually composed of aromatic rings while the end groups are typically composed of hydrocarbon chains. These end groups lower the melt temperature of a crystalline LC monomer by weakening the intermolecular attractive forces between the rigid rod cores in the solid state.

When an LC monomer is heated above the crystalline melt temperature, the individual LC monomers assemble into domains in which the molecules have a specific orientation. Depending on the specific system, there can be various mesophases that describe the relative orientation of the molecules. The nematic mesophase is the most common, and it is characterized by parallel orientation of the molecules in one dimension along the long axis, but no orientation with respect to the other axes. Orientational order increases to two dimensions in the smectic mesophase. The LC domains resemble solid crystals in orientational order but can flow like liquids, since they are above the crystalline melt temperature. These characteristics may result in anisotropic properties on the macro-level that exist in a defined temperature range [9]. When the temperature is increased beyond the LC mesophase range, the LC monomers lose all orientation and enter the isotropic phase. The temperature at which the monomer is polymerized locks in

the molecular orientation of the corresponding phase by cross-linking the monomers into a three-dimensional polymer network.

When crosslinked, or "cured", in the LC mesophase temperature region, the anisotropic order of the LC monomers is locked into the polymer network. The rigid rod structure of the LC molecules imparts desirable properties such as high stiffness, high Tg values (e.g. Tg > 300°C), and enhanced thermal stability to the polymer network. In addition to these properties, the LC domain boundaries act as a crack deflector and improve toughness when compared to the isotropic structure [10-12]. In recent years, the use of LC monomers for the formation of highly crosslinked networks has been examined for advanced composites and adhesives [13-18]. The LC monomer to be examined in this work is referred to as JNM-1 (Figure 1). This monomer contains two reactive acetylene groups as well as two terminal acrylate groups. The presence of both moieties gives it a "dual" curing capability [13,19]. Crosslinking of the monomers can proceed first through low temperature thermal or electron beam curing of the acrylate groups, followed by higher temperature curing of the acetylene groups. This dual curing capability allows increased flexibility in the processing of the material for various applications. In addition, JNM-1 exhibits a smectic LC mesophase between 48°C and 69°C. This phase is characterized by two-dimensional ordering and dense packing of the rigid rod monomers in planes. If curing is conducted while the monomer is in the LC phase, the resulting crosslinked structure is expected to possess enhanced toughness and reduced shrinkage in addition to a high glass transition temperature. A high glass transition temperature can also be achieved in the isotropic phase.

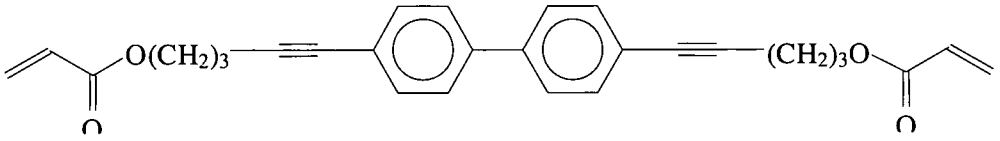

Figure 1: JNM-1 liquid crystal monomer structure

1.3.2 Importance of the Bond Interface

The primary goal in the adhesion process is to bond two materials together in order to provide a path for the transmission of force from the two materials through a third material called an adhesive. In the adhesion process, two main factors define the overall integrity and performance of the adhesive bond: the strength of the adhesive material and the strength of the adhesive-adherend interface. The adhesive material strength is a function of the chemical and physical nature of the material (cohesive forces). The strength of the adhesive-adherend interface is a function of many factors such as adherend surface energy, chemical composition, and surface roughness, as well as adhesive surface tension and degree of coupling to the adherend surface (adhesive forces). Proper adherend surface preparation is a crucial step in optimizing the adhesive-adherend interface. Effective surface preparation helps to create strong bonds at the adhesive-adherend interface that are stronger than the intermolecular bonds between the molecules of the adhesive bulk. In this case, the inherent strength of the adhesive becomes the defining factor in the overall strength of the adhesive bond, resulting in cohesive failure during testing. This type of failure occurs within the adhesive bulk and not along the adhesive-adherend interface. As noted previously, a primary goal of this study is to determine the conditions necessary to achieve cohesive failure for the LC adhesive and aluminum substrate system. When cohesive failure is achieved, the inherent strength of the LC material can be evaluated in order to guide further improvements in adhesive performance via synthesis and/or processing changes.

While the mechanical properties of an adhesive can be attributed to its chemical composition and state of cure, the properties of the adhesive-adherend interface are more complex in origin. In the ideal case the forces that represent the strength of the adhesive-adherend interface are generated by wetting of the adherend by the adhesive in the liquid state, followed by chemisorption. Chemisorption is the chemical reaction of an adhesive molocule with the molocules of the substrate surface to produce a molecular link between the two. Wetting is defined on a macroscopic level as full and complete coverage of a solid surface by a liquid. Incomplete coverage of the solid by the liquid (voids) leads to an uneven force distribution throughout the bondline, thereby reducing mechanical

properties. On a molecular level, the presence of voids indicates that the surface energy of the solid adherend is low relative to the surface energy of the liquid adhesive. Surface energy, or surface tension, is an indicator of the degree of molecular attraction within a substance. A quantitative measure of this surface energy is observed when a liquid drop assumes an equilibrium shape on the surface of a solid. The angle between the edge of this shape and the solid is called the contact angle and it is related to surface energy through Young's equation (Equation 1):

$$\sigma_{sv} - \sigma_{sl} = \sigma_{lv} \cos \theta \qquad (1)$$

The first term on the left (σ_{sv}) is the surface tension of the solid in equilibrium with the saturated vapor of the liquid, and the next term to the right (σ_{sl}) is the interfacial tension between the solid and the liquid. The first term on the right side of the equation (σ_{lv}) is the surface tension of the liquid in equilibrium with its saturated vapor and θ is the contact angle for the given liquid on the given solid. Good wetting of a surface corresponds to a small contact angle, which will occur in a system with a high solid surface energy and a low liquid surface energy. Surface energies can be measured through techniques such as inverse gas chromatography and contact angle measurements in order to evaluate the interfacial relationship between a liquid adhesive and a solid adherend. However, these techniques are very precise and complex and do not reveal the full range of factors that determine the interaction between the two mediums [4-6]. Consequently, the easiest way to determine the mechanical response of an adhesive/adherend system at this point in time is through destructive evaluation.

1.3.3 Substrate Surface Preparation

As noted previously, surface preparation is a process that changes the morphology and/or chemical composition of the surface of the adherend and is therefore an important factor in the development of an adhesive bond. A change in morphology may create a larger surface area for mechanical interlocking or simply serve to control the surface texture over the entire bondline. Surface preparation may be as simple as wiping a

surface with a solvent and gritpaper or as complex as an electrochemical etch. The surface treatment of aluminum for bonding in structural applications has been thoroughly studied in the past due to the extensive use of this material in the military and commercial aerospace industries [2,20-25]. The primary goal of those research efforts was to develop and/or analyze surface treatments that produced a controlled oxide layer on the surface of the aluminum, in order to promote strong adhesive-adherend interaction. Other goals of that body of research included improved resistance to moisture and humidity, which often weaken interface strengths. Many aluminum surface treatment methods involve chemical solutions that initially remove the aluminum oxide surface layer and then allow for a controlled re-growth of this layer. Other surface preparation methods serve to simply roughen and clean the surface. In order to effectively evaluate surface preparation results, it is necessary to understand the fundamentals of aluminum surface preparation.

Aluminum alloys such as 2024-T3 and 7075-T6 are used in most of the bonded metallic structures in aircraft, and therefore much of the aerospace surface preparation research has been performed on these materials [2]. When using aluminum for bonding, a minimum surface treatment of solvent cleaning is usually necessary to remove oils and debris that accumulate during the manufacturing and handling processes. However, this treatment does not modify the surface oxide morphology and only prevents surface contaminants from interfering with the adhesion process. Physical treatments of the aluminum produce better adhesion results, starting with the modification of the surface morphology. A roughened aluminum surface can be quickly and easily produced by gritblasting or hand abrading the surface to provide increased surface area for adhesion. "Scuff sand /solvent wipe" is a common surface preparation technique used on aluminum skins in the repair of military aircraft sandwich structures such as wings, especially in field repair situations [26]. However, this method does not provide the strength and environmental resistance achieved with other more involved methods.

Phosphoric acid anodizing (PAA) is a well-established method for altering the oxide layer morphology on aluminum. The PAA process was developed in response to a study of bond failures on aluminum by Bethune at Boeing Aircraft Corporation [27]. This study determined that the reason for interfacial failures and low shear strengths of

the samples was the morphology of the oxide layer produced by the FPL etch (a sulfuric acid/sodium dichromate etch) used up to that time to prepare the aluminum surface for bonding. Basically, the PAA process changes the way the oxide layer is produced. This process consists of an initial degreasing and cleansing step such as the FPL process, followed by anodization at 10V for 20 minutes in an aqueous solution containing 10% H_3PO_4 by weight. The PAA process produces a controlled oxide layer consisting of cellular and finger-like structures that provide porous regions much larger than the oxide structures formed by the FPL process. These structures are well suited for mechanical interlocking with an adhesive [20,21,24]. Further studies on the effectiveness of the PAA treatment showed that the resultant oxide layer is hydrolyzed by atmospheric moisture over time, which ultimately changes the oxide structure [24]. For this reason, it is standard procedure to bond the treated aluminum within approximately 8 hours following treatment. Other studies have shown that the initial cleansing step does not have to be the FPL etch, but can be any cleansing technique, such as the more environmentally friendly P2 etch (a sulfuric acid/ferric sulfate etch – ASTM D2651 [28]) or even hand abrasion [20]. The current standard for the PAA process is detailed in ASTM D3933-98 [21].

Primers and coupling agents are also used to modify the surface, in addition to the gritblasting and PAA treatments that provide regions for mechanical linking between the adherend and the adhesive. PAA treated aluminum is highly susceptible to oxide hydrolysis, and often a primer is applied to protect the surface. Also, certain primers protect the bondline from environmental exposure such as salt spray and humidity. A study using a corrosion-inhibiting epoxy phenolic primer called BR-127 (Cytec Fiberite, Inc.) showed that 95% strength was retained after 180 days exposure to salt spray in a set of primed 2024-T3 coupons bonded with an epoxy adhesive [2]. A different study of the same primer on PAA treated aluminum showed that the primer effectively coated the cellular and finger-like oxide structures of the surface, serving to protect the structure from hydrolysis and possibly promote penetration of the adhesive to maximize the degree of mechanical interlocking [22].

Silane treatment also has been used to alter the surfaces of metals or glass to provide an active bonding layer for coupling to other dissimilar materials. The chemical

structure of silanes allows for chemisorption with the oxide layer on the adherend and covalent or hydrogen bonding with the molecules of the adhesive. Typically silanes are used for polymer composite fiber and filler surface treatments. Research on using silanes for surface modification purposes is well documented [29] and will be discussed in more detail later.

CHAPTER II

EXPERIMENTAL PROCEDURE

2.1 Experimental Overview

A summary of the general experimental program of this study will clarify the direction of the individual experimental procedures used. In order to determine suitable cure cycles and understand their effects on the monomer, characteristic temperatures and morphologies of the adhesive material were identified using differential scanning calorimetry (DSC) and polarized light microscopy. Lap shear samples were used throughout the duration of the study to develop adhesive cure cycles and evaluate various surface preparations. One-inch by four-inch aluminum coupons were placed in custom aluminum jigs to fabricate individual lap shear coupons. This method will be discussed in detail later. Initially, lap shear samples were fabricated using simple surface preparations with a given amount of LC monomer along the bondline. These samples were cured according to various cure cycles and then pulled in tension to determine tensile lap shear strength. Once the cure cycles were developed, surface preparations were varied to determine their effect on the tensile lap shear strengths. Each of these experimental procedures is detailed in the following sections.

2.2 Development of Adhesive Cure Cycles

As noted above, DSC and polarized light microscopy were used to study polymerization reactions and phase transitions in JNM-1 monomer and the resulting polymers formed. DSC is a method to measure heat related changes within a material as a function of temperature and identify phase transition temperatures. A material phase transition is identified by an endothermic peak on a DSC thermogram. This event signifies the heat of fusion at the melting point or LC phase transitions. An LC monomer

will exhibit at least two endotherms upon heating: the transition from the solid crystalline phase to the LC mesophase and then the LC mesophase to the isotropic liquid phase. Heat of polymerization is identified by an exothermic peak on a DSC thermogram. Polarized light microscopy utilizes plane-polarizing filters to eliminate randomly polarized visible light when observing a sample. Assuming the sample is thin enough to transmit light, polarized light microscopy is used to reveal birefringence in the material. Birefringence is defined as the presence of direction-dependent refractive indices in a solid or liquid material. It is a property of materials with long-range molecular order, such as LC materials in the smectic or nematic mesophase, which causes the rotation of plane-polarized light. Birefringence is identified by a textured and usually colorful pattern under a polarizing light microscope. This pattern is formed by the rotation of polarized light as it passes through the material. The order of the LC molocules reveal a specific refractive index, however, the different regions of molecular order through the thickness of the material cause a change in the rotation of the polarized light. The different regions of molecular order, therefore, are revealed by the changes in color in the material. Isotropic materials exhibit no molecular order, and therefore do not transmit polarized light. The combination of DSC and polarized light microscopy techniques gives strong evidence about the LC phase transitions and the properties of the monomer in different phases.

JNM-1 monomer compounded with 1% benzoyl peroxide by weight was used as the adhesive composition for this research. Benzoyl peroxide acts as a thermal initiator for the polymerization reaction of JNM-1. The benzoyl peroxide was solution-mixed and freeze dried with the JNM-1 in order to achieve homogeneity. With no added initiator, JNM-1 polymerizes around 250°C. At 1 wt% concentration, the benzoyl peroxide lowers the peak reaction temperature to approximately 112°C. The polymerization temperature ranges are identified by exotherms in the DSC thermograms as shown in Figure 2. The DSC instrument used in this experiment was a TA Instruments 2910 DSC, operated at a heating rate of 5°C/min with an inert atmosphere.

Cure cycles were evaluated through DSC thermograms, visual observation, and polarized light microscopy. DSC data on the cured polymer were obtained from cured

lap shear samples. The cured polymer was shaved off from the coupon "flash" outside the bondline, where some of the material had pressed out during the cure cycle. It was assumed that surface preparation had no effect on the DSC data. DSC data taken before and after cure were compared to ensure that the monomer had completely polymerized and the residual cure exotherm had been significantly reduced (Section 3.1, Figure 7, p 22). The cured polymer was also evaluated after each cure cycle for color and consistency differences, which were found to be related to the specific cure temperatures and the post-cure temperatures applied. Polarized light microscopy was used to verify the phase morphology of the polymer during cure. A thin film of the monomer was cast on a glass slide and heated to observe the polymer texture as cure progressed. A Nikon polarizing microscope was used to verify the phases. A previous study provided much insight into the cure characteristics of the neat resin of JNM-1 and was used to help formulate the cure cycles for the lap shear samples [30].

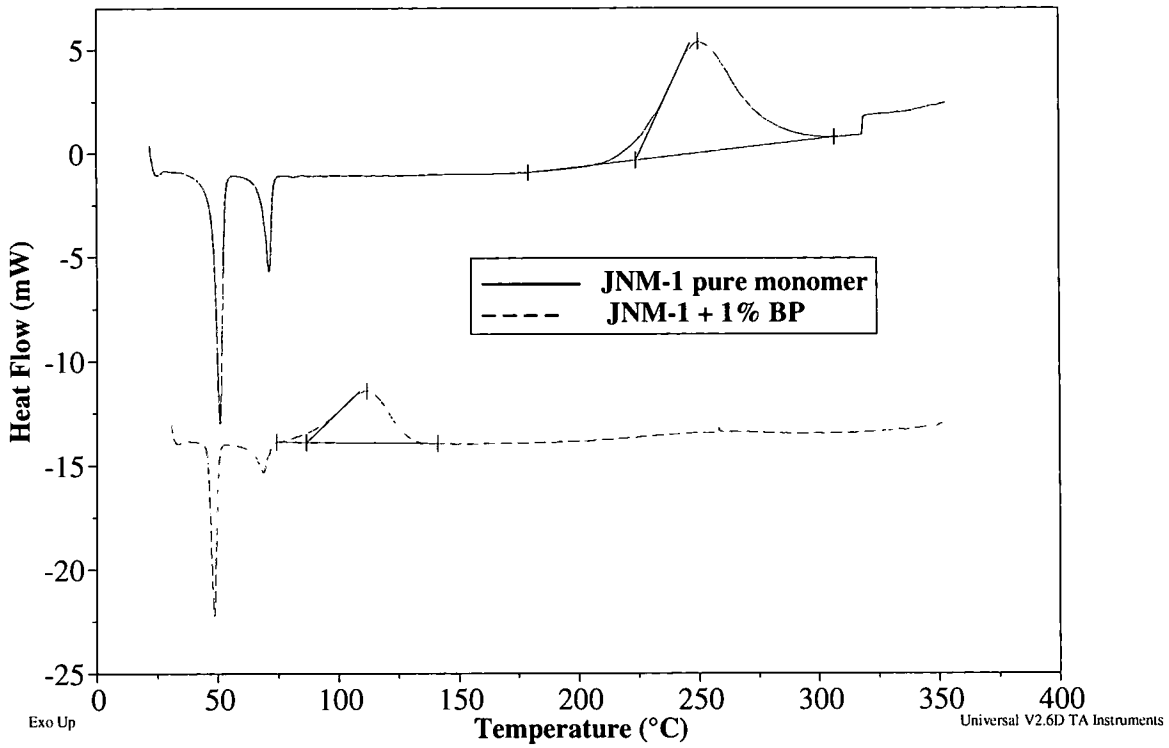

Figure 2: DSC thermograms illustrating the effect of 1% benzoyl peroxide (BP) initator in shifting the main cure reaction to a lower temperature. Heating rate = 5°C/min; argon atmosphere

2.3 Development of Surface Preparation Techniques

Surface preparation was classified into two categories: basic surface treatment to modify surface morphology (grit blasting or PAA treatment) and subsequent surface chemical treatment (silane or BR®-127 primer). The basic surface treatments were evaluated independently and in various combinations, as given in Table 1.

Table 1: Test matrix for surface preparation variables

Condition #	Surface Morphology	Surface Chemical Treatment
1	Gritblast/Solvent Wipe	None
2	Gritblast/Solvent Wipe	2% silane solution
3	Gritblast/Solvent Wipe	4% silane solution
4	PAA	None
5	PAA	2% silane solution
6	PAA	4% silane solution
7	PAA	BR®-127 primer

Gritblasting served as the baseline surface preparation, and it is representative of the military "scuff sand/solvent wipe" procedure mentioned previously. This procedure is the quickest and easiest of all the surface preparation procedures. Initially, the aluminum coupons were held 1" below a gritblasting nozzle for 10 seconds. After gritblasting, residual grit was blown away with a high-pressure air stream and the bondline was wiped gently with an ethanol-soaked Kimwipe. The coupon was then placed in a plastic bag until future use. The gritblasting apparatus used was a Ruemelin Type DC2020 device set at an air pressure of 50 psi. The grit media were Ballotini® glass impact beads, size AD (106-212 microns nominal diameter). The gritblasting was performed shortly before lap shear assembly or further treatment to avoid contamination.

PAA treatment was performed according to ASTM Standard D3933-98 [21]. The PAA process is a standard surface treatment in the aerospace industry when aluminum is bonded. The process consists of immersing the individual lap shear tabs for five minutes

in hot alkaline solution followed by a five-minute rinse with room temperature deionized (DI) water. In this work the alkaline solution was Turco 4215, a borate and phosphate based cleaner for spray and immersion applications, held at 60-70°C. The tabs were then inspected for the absence of water breaks on the surface, and then placed in a cleansing solution. Water breaks are discontinuities in a flowing water film across the surface of the substrate and indicate differences in substrate surface characteristics. If water breaks were detected, the entire PAA process was restarted. The cleansing solution used was P2 etch, which is a solution of sulfuric acid (36% by weight) and ferric sulfate (165 g/L) held at 66-71°C. The tabs were left in the etchant for ten minutes and then inspected for the absence of water breaks again. If no water breaks were present, the tabs were rinsed with DI water for five minutes. Following this rinse, the tabs were attached to aluminum clips and suspended in a bath containing a 10% by weight phosphoric acid solution. The anodizing step was accomplished by applying an electrical potential of 10 V across the tabs for twenty minutes. Anodizing is a means of building an aluminum oxide film on the surface of aluminum by accelerated and uniform hydrolysis (oxygen release and reaction with aluminum).

The tabs were then rinsed for five minutes in DI water and placed in an oven at 60°C until dry (approximately fifteen minutes). Throughout the PAA process, the tabs were not allowed to dry until the final step. This is a crucial requirement for the success of the process. All PAA samples not coated with primer were assembled in the lap shear jigs within four hours of treatment to ensure minimal environmental exposure. Primed coupons did not require this time constraint because of their increased resistance to oxidation and hydrolysis.

Silane coupling agents were applied to gritblasted tabs as well as tabs treated by PAA. Two silanes, SIM 6487.3 and SIM 6487.4, were acquired from Gelest, Inc. The chemical structures of these silanes are shown in Figure 3. These methacrylate compounds were chosen because of their potential chemical reactivity with the acrylate groups of JNM-1.

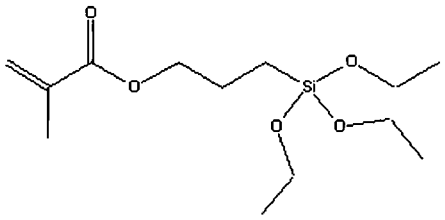

Methacryloxypropyltriethoxy silane
Gelest SIM 6487.3

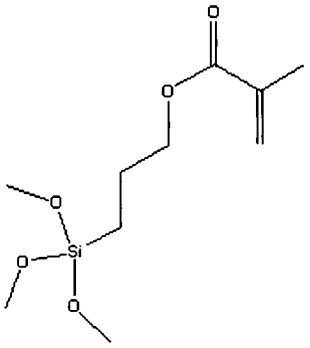

Methacryloxypropyltrimethoxy silane
Gelest SIM 6487.4

Figure 3: Chemical Structures of Silane Coupling Agents

Preliminary research through contact angle analysis indicated better wetting results with isotropic JNM-1 on aluminum with an application of SIM 6487.3 versus an application of SIM 6487.4. Based on these findings, SIM 6487.3 was selected as the primary coupling agent to be used for this study.

Application of the silane coupling agent was performed using a process suggested by the manufacturer. A 95% ethanol / 5% water (vol.) solution was adjusted to pH 5.0 with acetic acid. Silane was added with stirring to yield the desired weight concentration. The solution was then stirred for five minutes to allow for hydrolysis. Lap shear tabs were either gritblasted or PAA treated immediately before silane application. After hydrolysis, the tabs were each placed in separate containers of the solution and manually agitated for two minutes. The tabs were then rinsed with a brief dip in ethanol and placed in a 110°C oven for 15 minutes to cure the silane layer. After the silane cure, the tabs were placed in the lap shear jig for assembly. Even though the lap shear bondline is 1/2", approximately 1" at the end of each tab was treated to ensure full coverage. The silane application procedure is discussed more thoroughly in the following section.

Finally, BR® 127 Corrosion Inhibiting Primer (a modified epoxy phenolic) was applied to certain tabs that were initially treated by the PAA process. The primer was brushed on at room temperature onto tabs that had just been PAA treated. The primer thickness was between 0.0025 mm and 0.0075 mm (based on previous application experience). After the primer was applied, the tabs were left to air dry for 30 minutes.

The tabs were then cured in an oven for 30 minutes at 120°C. After this, the tabs were allowed to cool and were wrapped in clean cotton cloth for protection against dust and dirt. According to the manufacturer's claims, a surface protected with BR-127 primer has an indefinite shelf life. In this study, all primed tabs were used within one month of the priming date.

2.4 Silane Application Process – Dissolution Method

The silane application process that was used throughout this study was the process that was recommended by the manufacturer, as noted previously. However, an investigation into the literature revealed many variables in the application process that could produce different results. Silanes may be applied by various processes, but all follow the same general reactive steps in bonding to a substrate. Many widely used organosilanes, including the silane used in this study, have one organic substituent and take the form,

$$R'—Si(OR)_3$$

where R is an alkyl group and R' is the organic functional group designed to react with an adhesive. The first step in the application of these silanes is hydrolysis of the three silicate groups (SiOR) to form silanols (SiOH). Condensation follows to form siloxane oligomers, which then hydrogen bond with OH groups of the substrate. Finally, a thermal cure forms covalent bonds with the substrate by removing water. The thickness of the polysiloxane layer on the substrate is determined mainly by the concentration of the applied silane solution. Typically, a monolayer coverage is desired in order to optimize the "link" between the adhesive and the adherend. In most cases, however, a polysiloxane multilayer develops which reduces the strength of the link [31,32]. Studies of the silane application procedure show that there is an optimal silane treatment concentration for a given substrate that will produce a polysiloxane monolayer on the surface, and theoretically lead to better adhesion [33-36].

The optimal silane treatment can be determined from a set of experiments referred to as the dissolution method. This method is performed initially by treating a set of

substrate samples with increasing amounts of silane using the same application procedure. After treatment, the samples are individually exposed to a strong solvent for the silane for a given period of time. The concentration of silane extracted by the solvent is then measured using UV or IR spectroscopy and compared to calibration curves made using known concentrations of the silane in the solvent. This experiment is based on the theory that multilayers of the polysiloxane are not firmly attached to the substrate and can be dissolved off by an appropriate solvent. This method was used by Fekete [33,34], Demjen [35], and Gulyas [36] to determine monolayer coverage concentrations of two different coupling agents on particulate mineral fillers. These fillers were then used in composites to see how the properties of the composites were modified.

A similar dissolution method was used in this study to determine the optimal silane concentration required to produce a polysiloxane monolayer on aluminum. First, the solubility of SIM 6784.3 silane was visually observed in dichloromethane. Then, a calibration curve was constructed by measuring the magnitude of the characteristic absorbance peak of the silane through FTIR for increasing concentrations of silane in dichloromethane. The characteristic IR absorption peak of the silane occurs at 1710 cm^{-1}, which is actually the IR absorbance caused by the -C=0 group of the molocule. Next, nine 1" wide lap shear tabs were PAA treated and then treated with increasing silane concentrations (1, 2, 4, 6, 7.5, 8, 10, 15% by weight) according to the aforementioned silane application procedure. These tabs were then placed in individual plastic containers with known amounts of dichloromethane. The containers were closed and placed in a refrigerator for 48 hours to minimize evaporation of the solvent. The containers were removed from the refrigerator and the substrates were then removed from each container. The concentration of residual silane in the solvent was measured by FTIR.

To verify the results of the first trial, a second trial was performed. The substrates for this trial were 1 in. wide aluminum lap shear tabs with slots cut into the side across most of the width of each tab along 2.5 in. of the tab's length as shown in Figure 4.

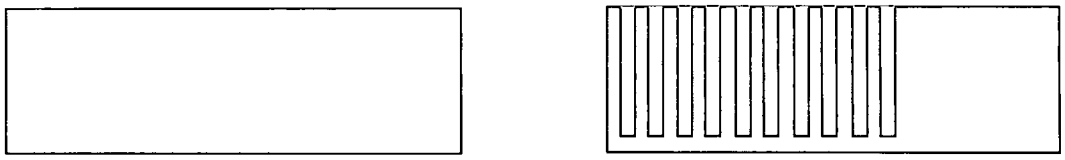

Figure 4: Comparison of Tabs Used For the Dissolution Method

All 2.5 in. of each slotted aluminum tab was treated with silane, as opposed to only ~1 in. for the standard procedure. The reasoning for this change was to provide more surface area for the silane to bond to, effectively introducing more silane into the system. With more silane in the system, the presence of siloxane multilayers would theoretically be easier to detect due to an increased concentration of residual silane in the solvent. Four slotted tabs were treated individually by PAA and then with increasing concentrations of silane (1, 3, 5, 10% by weight) in the same manner as before. These tabs were then placed in glass jars containing known amounts of dichloromethane and capped. The tabs were exposed to the dichloromethane at room temperature for 48 hours and then removed from the solvent. The concentration of silane in the solvent from each jar was then measured by FTIR. The FTIR used for the concentration measurements was a Nicolet 20DXB FTIR Spectrometer with a standard NaCl sample cell.

2.5 Lap Shear Coupon Fabrication and Testing

All lap shear specimens were prepared using 2024-T3 aluminum as the adherend and JNM-1 monomer compounded with 1% benzoyl peroxide by weight as the adhesive. Lap shear samples were prepared for various surface preparations and cure cycles in accordance with a modified version of ASTM Standard D1002 [37] (description follows). A fiber-glass cloth scrim also was used in the bondline to assist in achieving consistent gap thickness and to act as a containment device for the adhesive in the liquid state. For each sample, the jig and coupons were heated to 80°C for at least 20 minutes in a programmable press before the monomer powder was placed on the bondline. Approximately 0.032 g of monomer powder was placed on the overlap region on each coupon and liquefied at 80°C. The remaining top side coupons then were placed in position and the jig was assembled completely. After the jig was prepared, the press was

closed and the specific cure cycle was started. All samples were cured at a pressure of 0.394 MPa (57 psi) regardless of cure cycle. This pressure was used

After the cure cycle was completed, the jig was allowed to cool to room temperature before the lap shear samples were removed. Each sample was tested for lap shear strength according to ASTM Standard D1002. Ten lap shear coupons were fabricated for each surface preparation condition given in Table 1. For each condition, five coupons were cured in the isotropic phase using an isotropic cure cycle, while five were cured in the LC phase using an LC cure cycle. The programmable press used in these experiments was a Tetrahedron MTP Press, Model 1301 with precision temperature and pressure control capabilities.

The modification to the ASTM lap shear standard was the use of individually prepared 1 in. wide coupons rather than the preparation of one 7 in. wide bonded sheet to be subsequently cut into 1 in. wide coupons. Lap shear samples were assembled in a custom-built jig (Figure 5) to ensure coupon alignment and a bondline gap between 0.05 mm and 0.125 mm. The rationale for this modification was the need for quicker testing during many iterations of cure cycle and surface preparation development. In order to determine the effect of the modified method on lap shear results, the standard ASTM method was used to fabricate ten lap shear coupons using the same surface preparation and adhesive setup as a set of samples prepared using the modified procedure. For this comparison, two sets of 7 in. 2024-T3 aluminum plates were prepared using the PAA process followed by an application of BR-127 primer. These plates were bonded using an amount of monomer proportional to the size of the bondline with the 1 in.tabs. One set of plates was cured using the LC cure cycle, while the other was cured using the isotropic cure cycle. Both sets were cured in the programmable press at the same pressure as the modified tabs. The resultant tabs were then tested to determine their lap shear strength and failure mode for comparison to similar tabs from the modified fabrication method.

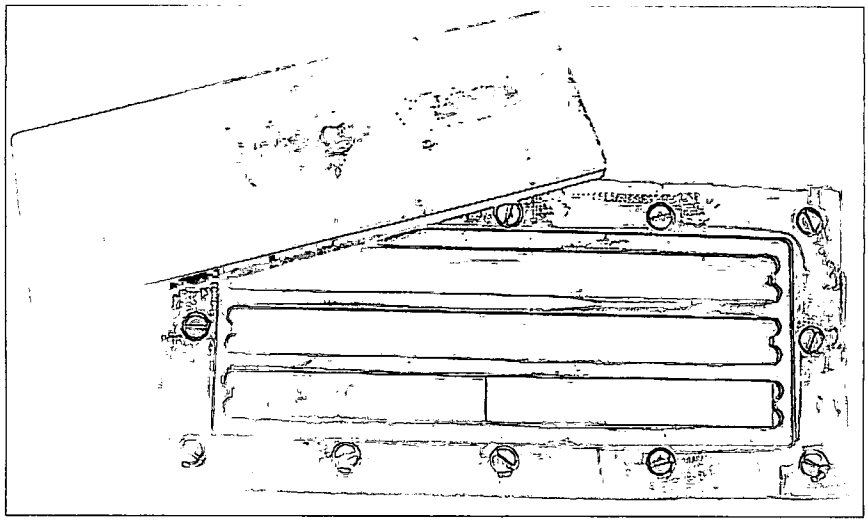

Figure 5: Custom Jig Used for Lap Shear Coupon Fabrication

CHAPTER III

RESULTS AND DISCUSSION

3.1 Cure Cycle Development and Analysis

Two cure cycles were developed to polymerize the JNM-1 monomer: an isotropic phase cure cycle and an LC phase cure cycle. These cure cycles are illustrated in Figure 6. The temperature ranges for each cure cycle were determined by initial inspection of the DSC thermogram for JNM-1 monomer with 1% BP by weight, shown in Figure 7. This curve shows that the monomer is crystalline at room temperature and melts from a solid crystalline phase to a liquid crystalline (smectic) phase at 48°C, as indicated by the first endothermic peak. A second endothermic peak at 69°C indicates a transition to the isotropic liquid phase. The exothermic peak centered at 112°C represents the main polymerization reaction, with an apparent reaction onset temperature of 75°C.

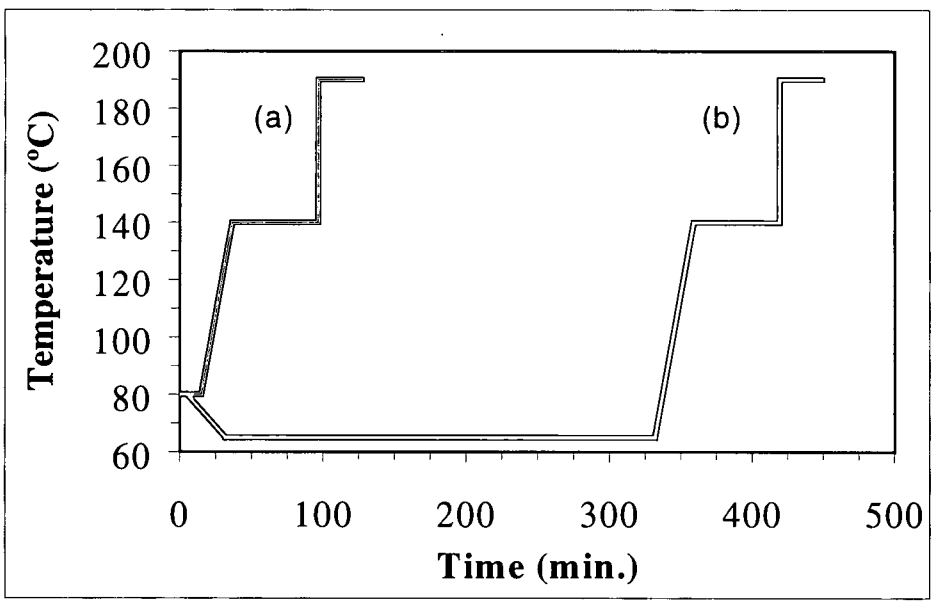

Figure 6: Cure cycles selected for JNM-1 in the a) isotropic and b) LC phase

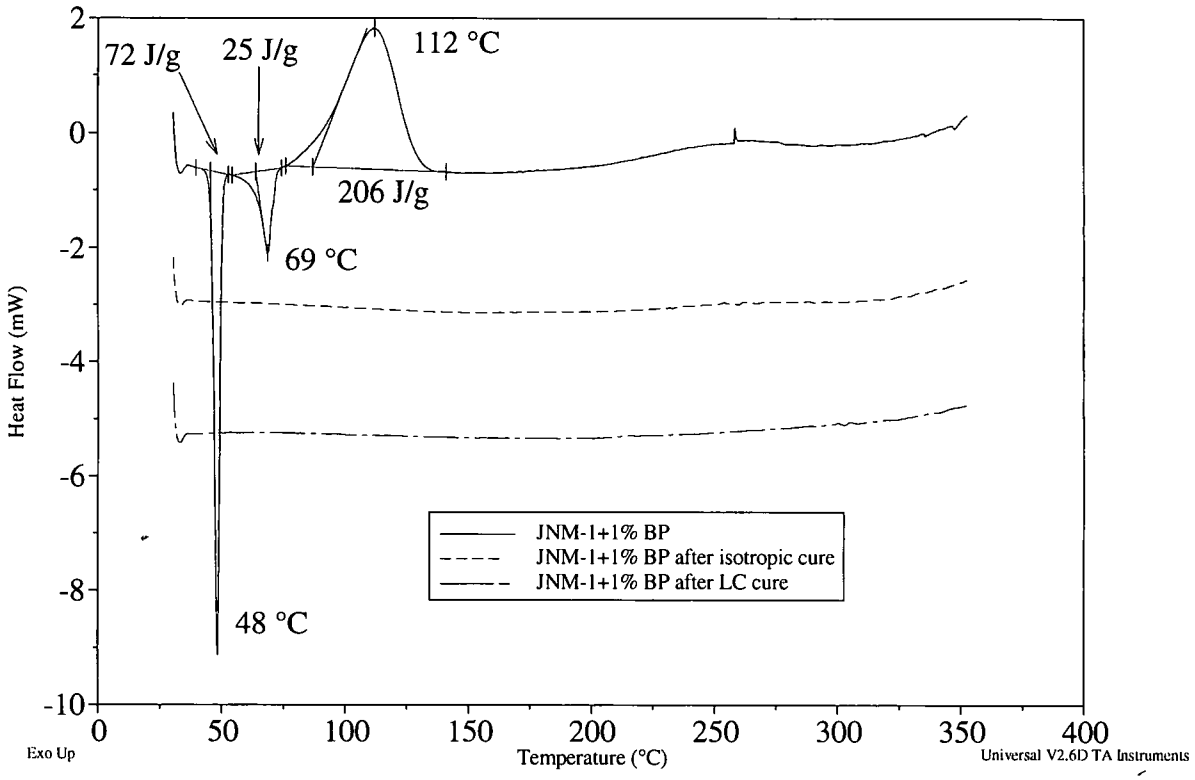

Figure 7: DSC thermograms illustrating the progress of cure for JNM-1 with 1% benzoyl peroxide (BP); The upper curve is for an uncured sample, while the other curves are for samples cured following the two cure paths illustrated in Figure 6.

Based on these temperatures, an isotropic phase cure cycle was developed by heating the monomer at a temperature of 80°C for 15 minutes, which allowed the monomer to liquefy and wet the adherend, followed by a slow (2.8°C/min) ramp to an isothermal hold at 140°C for one hour. The necessity of a high temperature post-cure for achieving high temperature mechanical integrity of the polymer was determined in a previous study [30]. Therefore, a post-cure of 190°C for 30 minutes was added to the cure cycle to promote further reaction and thereby increase crosslink density.

An LC phase cure cycle was also developed using the initial DSC thermogram and data from the same previous study [30]. This cycle began with a five minute hold at 80°C, which allowed the monomer to liquefy and wet the adherend, followed by a very slow (0.6°C/min) cooling ramp to 65°C to allow for proper formation of the LC domains. The material was then held at this temperature for five hours to allow for sufficient

reaction to "lock in" the LC morphology. The isothermal hold was followed by the same post-cure cycle employed in the isotropic cycle: the material was heated to 140°C and held for one hour, then heated to 190°C for 30 minutes. Polarized light microscopy on cast thin films was used to confirm that a five hour isothermal hold at 65°C effectively locked in the LC morphology. While it was not confirmed in this study, it is believed that a shorter isothermal hold at 65°C would produce similar results.

To verify that the reaction had achieved a high degree of cure, a DSC thermogram of the cured material was analyzed. Figure 7 shows the DSC thermogram comparison between uncured JNM-1, JNM-1 that was cured in the isotropic phase, and JNM-1 that was cured in the LC phase. The disappearance of the endothermic peaks in these curves indicates that the polymer has been "locked in" to the morphology that developed prior to the cure reaction. Also, the significant reduction in the area under the exothermic peak indicates that the reaction achieved a high degree of conversion.

Photomicrographs of cured thin films of JNM-1 were obtained by polarized light microscopy. The isotropic cure cycle sample blocked all the polarized light and produced a dark picture, indicating an isotropic morphology. The birefringent texture of Figure 8 illustrates the various LC domains throughout the film, which allow polarized light to pass through.

3.2 Dissolution Method Results

The concentration of silane in solvent for the dissolution method was measured by FTIR 48 hours after the treated tabs were placed in the dichloromethane solvent. For the first trial, no silane was detected by FTIR for all nine treatment concentrations (1, 2, 4, 6, 7.5, 8, 10, 15% by weight). The second trial produced the same results as the first trial for all four concentrations (1, 3, 5, 10% by weight). While the absence of silane in solution was not expected, insight into the silane application procedure may explain this result.

Figure 8: Polarized optical photomicrograph of a thin film of JNM-1 with 1% BP, cured in the LC phase (100X)

Initially, a given amount of silane is mixed with ethanol solution for five minutes to allow for hydrolysis. Pluedemann [29] and Arkles [32] state that alkoxysilanes hydrolyze rapidly under mildly acidic conditions. Therefore, five minutes is most likely sufficient time to allow for full conversion of silane to silanol. The tabs are then placed in the hydrolyzed solution and gently mixed for two minutes so that the silanol molecules can condense and hydrogen bond with the hydroxyl groups of the aluminum surface. Pluedemann also states that the condensation of silanols to polymeric siloxanols is slow compared to hydrolysis. Other research on silane treatment of mineral fillers [33-36] allowed a longer mixing time with the silane solution, and yielded observable results. Therefore, the two-minute mixing time used in this work may not have been sufficient to allow for a high degree of condensation and hydrogen bonding of the silane to the aluminum. Following the mixing step, the treated substrates were dipped in alcohol. This action most likely removed some of the silane on the aluminum present in a multilayer or weakly attached to the aluminum.

After the alcohol dip, the treated tabs were cured for 15 minutes at 110°C. Silane theory states that polymer siloxanes that are hydrogen-bonded will bond covalently to the aluminum and to each other during this cure to form a relatively open polysiloxane network. A study by Sung [38], however, showed that the degree of cross-linking of the polysiloxane network is a function of the cure temperature. At higher temperatures, the polysiloxane network may become highly crosslinked and prevent penetration by an adhesive. This also may cause any silane multilayers that are present to link with the layer attached to the substrate. These factors reveal some of the potential problems with the silane manufacturer's recommended application procedure. Though the dissolution method results do not reveal an optimum silane treatment concentration for this system, silane treatment was used for lap shear samples to see if the coupling agent had any effect on lap shear strength.

3.3 Lap Shear Testing Results

3.3.1 Effect of Failure Mode on Lap Shear Strength

Two different types of failure modes were revealed during testing of the lap shear coupons. Adhesive failure of the bond occurs at the adhesive-adherend interface and allows for total separation of the adhesive from the adherend. Adhesive failure in this study was recognized as a clean separation of the adhesive scrim from all or parts of the two aluminum tabs in each coupon. The surface of the adhesively failed area was smooth. Cohesive failure of the bond occurs within the adhesive bulk and reveals the strength of the adhesive. Coupons that failed cohesively in this study were recognized by bits of scrim and adhesive covering the bondline on both tabs. A cohesive failure coupon and an adhesive failure coupon are shown in Figure 9 for comparison.

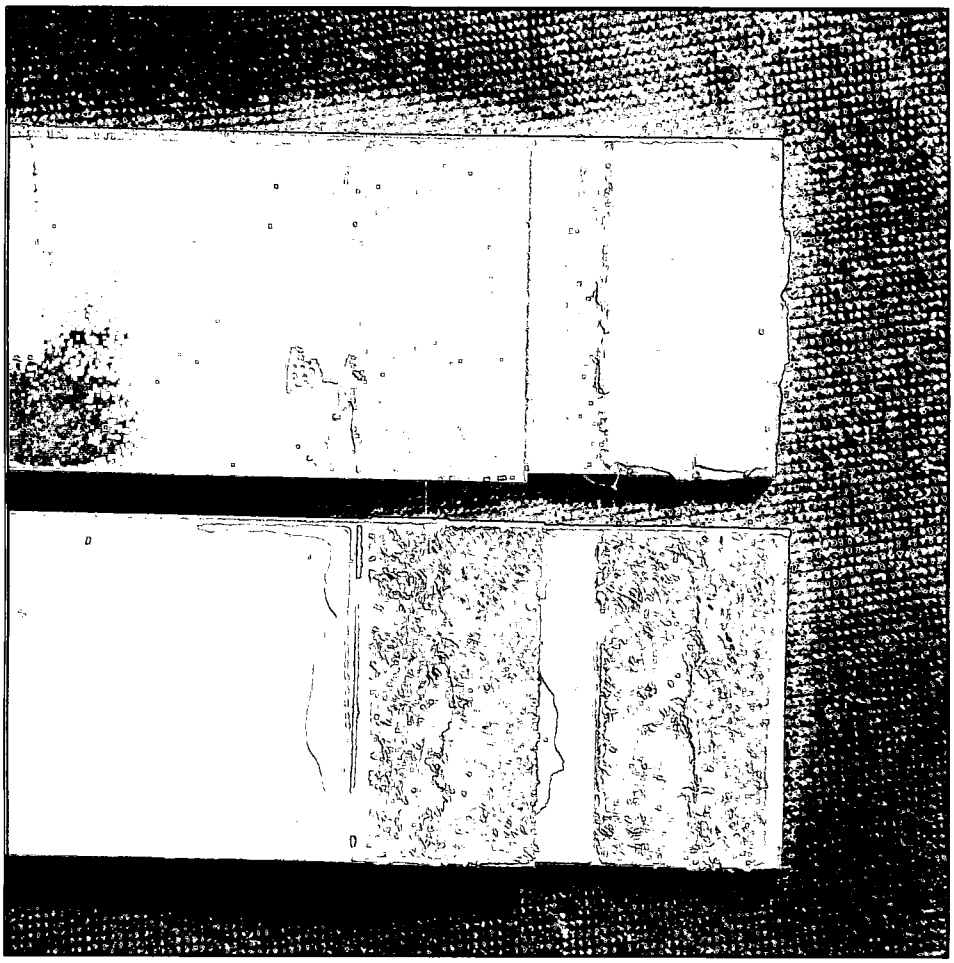

Figure 9: Lap shear coupons; the top coupon exhibits adhesive failure while the bottom coupon exhibits cohesive failure.

With some coupons, it was not immediately obvious what failure mode was revealed. For example, some coupons showed a failure mode with a scattered pattern of scrim and adhesive across the bondline or separation of the scrim completely from one tab with some adhesive left on that tab. However, in all of these cases the scrim and/or adhesive on each tab could be seen and touched to verify that the aluminum surface was not smooth like those coupons exhibiting adhesive failure. For this reason, these coupons were all classified as cohesive failure samples. There was no consistent trend with regard to the variations in cohesive failure samples when compared to surface treatment and cure cycle. This variation even appeared within a set of samples with the same surface treatment and cure cycle in some cases. Examples of the different types of cohesive

failure are shown in Figure 10. This variation in cohesive failure pattern is an indicator that the adhesive was not able to wet the adherend evenly across the bondline in some cases. This uneven coverage might be caused by minor differences in surface treatment across the bondline. In this case, these differences may be reduced by paying more attention to small details in surface treatment procedures such as handling time between tab treatment and coupon fabrication. The uneven coverage may also be caused by uneven pressure distribution during curing and non-repeatable flow patterns.

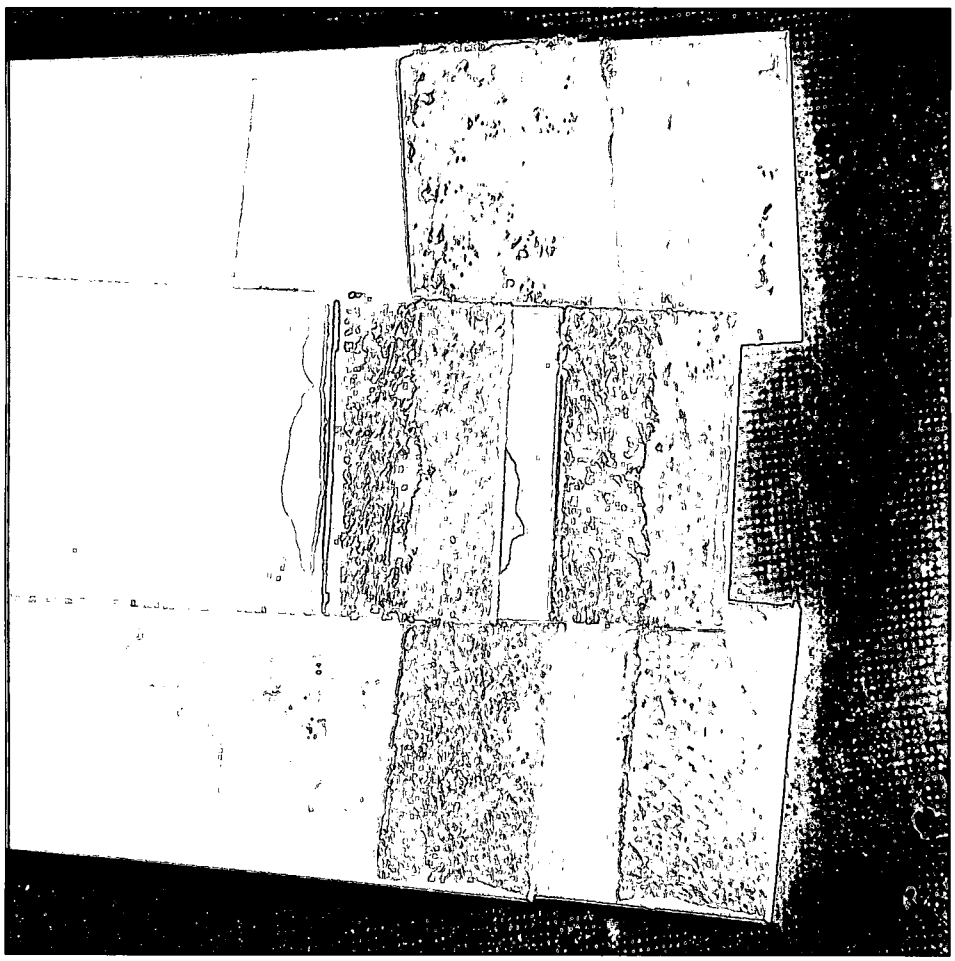

Figure 10: Variations in scrim and adhesive patterns for samples showing cohesive failure

There is a clear correlation between failure mode, lap shear strength, and initial surface treatment (PAA or gritblasting). All of the tabs treated by gritblasting (alone or

in combination with silane) failed adhesively and produced relatively low lap shear strengths. All of the tabs treated by PAA (alone or in combination with silane or BR-127) failed cohesively and produced higher lap shear strengths. In order to evaluate this contrast, the lap shear strength values for all surface treatments and both cure conditions were grouped according to initial surface treatment. This grouping also correlated with failure mode. These values were then averaged to compare the difference in lap shear strength as a function of failure mode and initial surface treatment. This comparison is shown in Figure 11. The standard deviation for each set of values is shown by the error bars on the graph. In both sets, the standard deviation is ± ~200 psi.

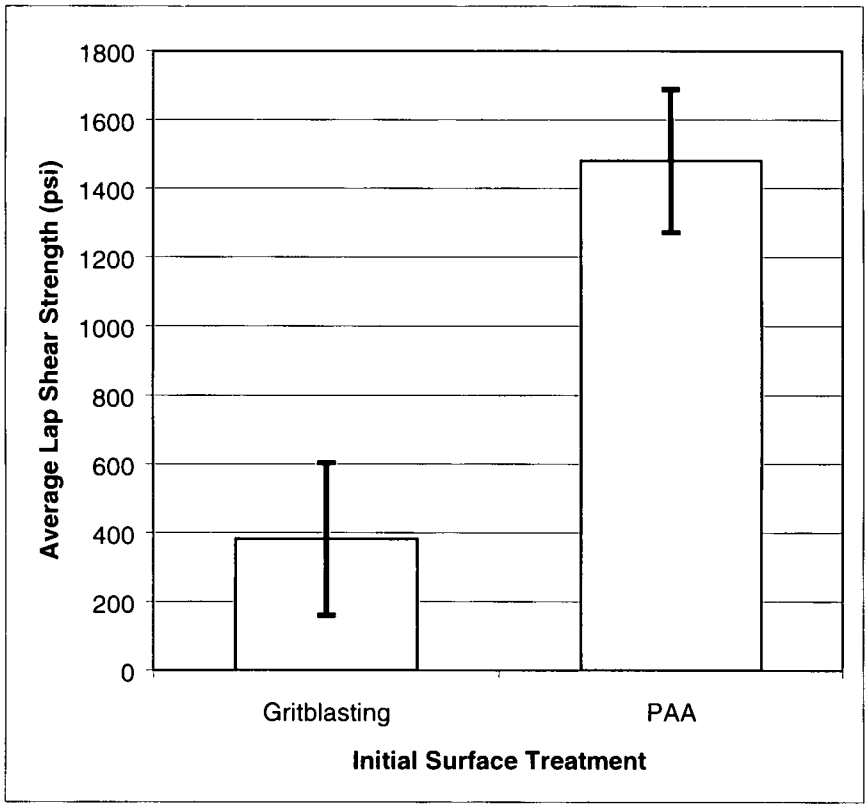

Figure 11: Comparison of initial surface treatment to average lap shear strength

Figure 11 illustrates the correlation between initial surface treatment (related to failure mode) and lap shear strength. Cohesive failure is obtained by treating the tabs initially with PAA. A higher degree of interaction between JNM-1 and PAA treated surfaces is demonstrated through this type of failure. This high degree of interaction

causes failure within the adhesive to produce relatively high lap shear strengths. Conversely, adhesive failure is realized by initially gritblasting the tabs. The adhesive failure of these coupons reveals a low degree of interaction between JNM-1 and gritblasted surfaces. Low lap shear strengths for gritblasted surfaces result from this poor interaction.

Clearly, the interaction between PAA treated aluminum and JNM-1 is much greater than the interaction involving gritblasted aluminum. The porous cellular structure of PAA treated aluminum enables a high degree of mechanical linkage while the large surface area provides ample area for chemisorption. A micrograph and illustration of the oxide layer of PAA treated aluminum are shown in Figure 12. The roughened surface of gritblasted aluminum has a relatively small surface area, since the surface topography is not as porous or structured as the PAA treated surface . Therefore, the JNM-1 does not penetrate and react with the aluminum surface to the same degree as with PAA treatment. These differences in surface structure are the cause of the different modes of bond failure and ultimately the difference in lap shear strengths.

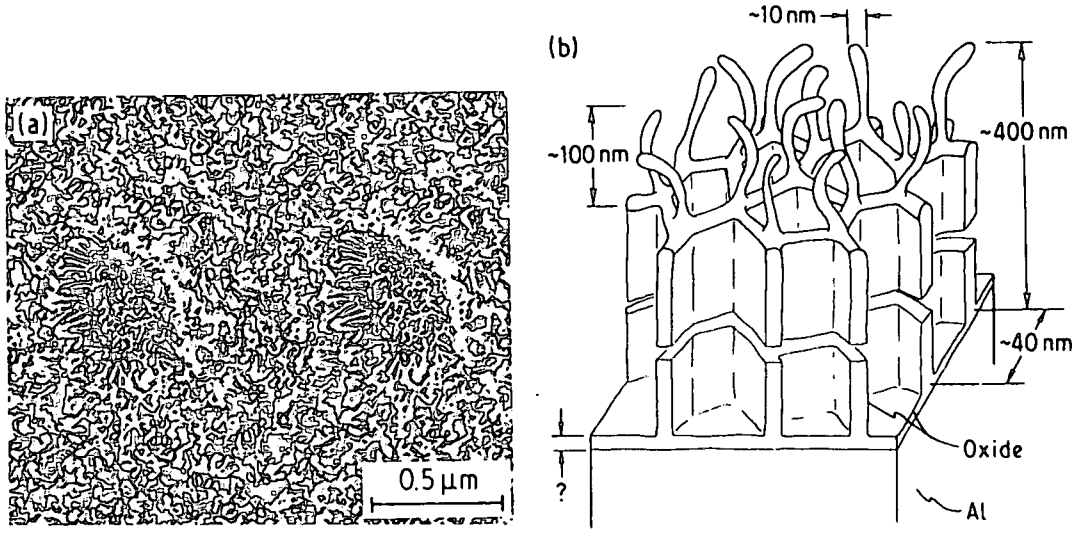

Figure 12: Stereo micrograph (a) and isometric illustration (b) of the oxide layer of PAA treated aluminum [39]

3.3.2 Effect of Silane Treatment and Cure Cycle on Lap Shear Strength

Silane treatment was used on the aluminum substrates in an attempt to form a coupling link between the aluminum oxide surface and the reactive acrylate groups of the JNM-1 monomer. Although the dissolution method did not reveal an optimum (monolayer coverage) treatment concentration, silane was applied to some of the aluminum tabs to see if there was any resultant effect on lap shear strength. Figure 13 shows the average lap shear strengths for coupons with initial gritblasting and PAA treatments followed by treatment with increasing silane concentration.

Lap shear strength increased with increasing silane concentration for gritblasted samples cured in the isotropic phase. However, scatter in the data makes this impossible to conclude with confidence. This trend was not realized for similarly treated samples cured in the LC phase. For samples treated with PAA, lap shear strength decreased to a relatively constant level for all silane treatments on samples cured in the LC phase. The average lap shear strength of these LC cured samples was approximately 25 percent less than the average lap shear strength for the corresponding PAA-only treated samples. This shows that silane treatment had an adverse effect on lap shear strength and did not serve to couple the aluminum with the LC-phase JNM-1. On the other hand, for similar samples cured in the isotropic state the maximum strength was obtained for 2% silane.

The causes of the varying effect of silane treatment on lap shear strength may be rooted in the silane treatment procedure. As noted previously, high cure temperatures for silanes most likely result in the formation of a highly crosslinked silane network on the surface. This network could effectively block the surface and prevent penetration of the JNM-1 monomer into the porous structure formed by PAA treatment, especially for the higher viscosity LC phase. This would inhibit the interaction of the JNM-1 monomer with the PAA treated surface and correspondingly decrease lap shear strengths. The high temperature used for silane cure in this study would produce such an inhibitive network. Also, the polymerization of the silanes could prevent reaction of the acrylate groups on the silane with the acrylate groups of the JNM-1 monomer. If the surface silane already reacted during the silane cure, the acrylate groups would not be available (exposed) at the interface. The surface blocking and functional group polymerization are most likely the

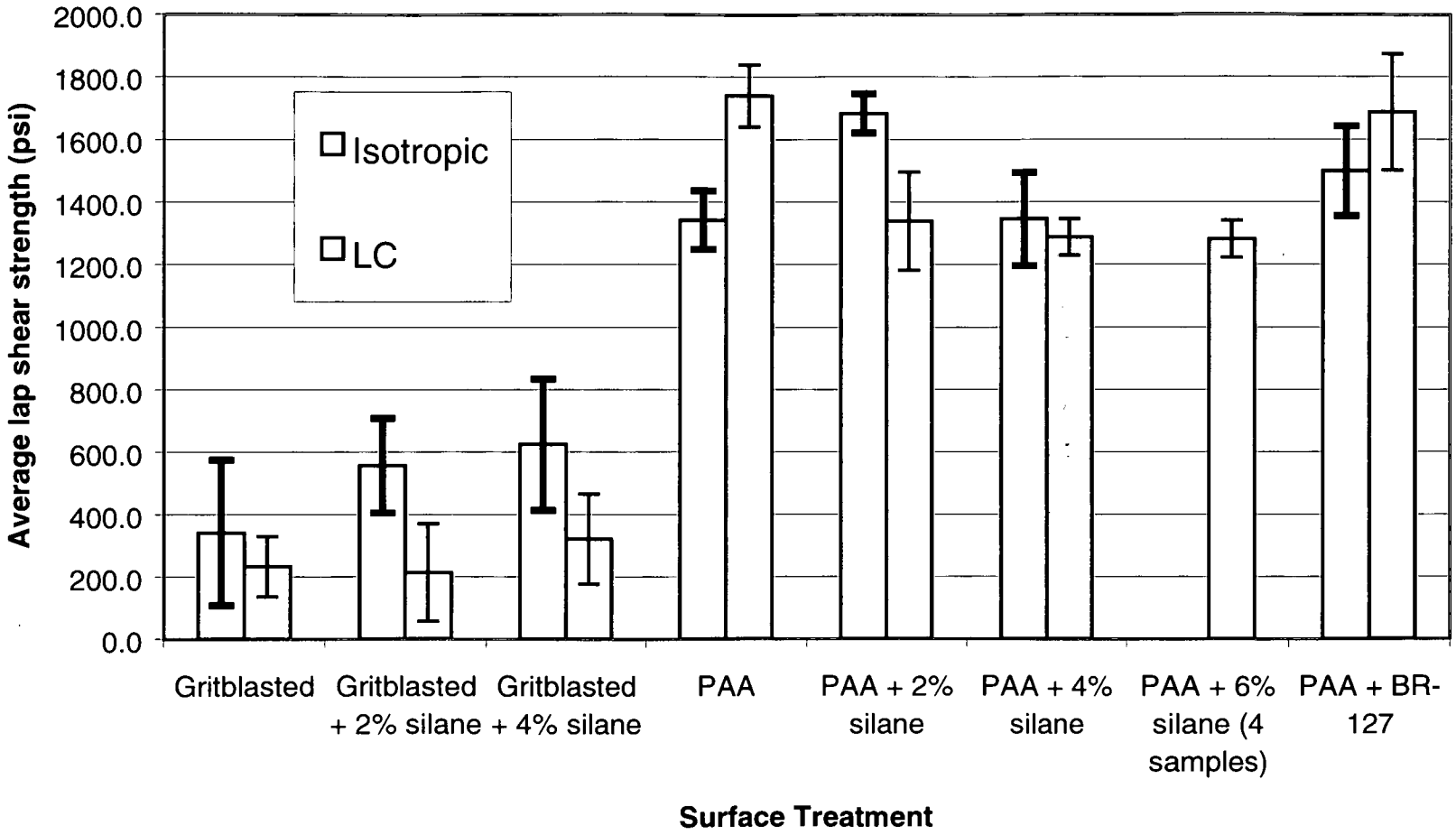

Figure 13: Comparison of surface treatment and cure conditions to average lap shear strength

reasons for lowered lap shear strengths with silane treatment. The results from the dissolution method are consistent with the hypothesis of a highly crosslinked silane network. These results showed that no detectable silane was present in solvent after immersion for 48 hours. This suggests that all of the silane molocules on the surface were linked tightly and could not be dissolved away. The combination of the lap shear and dissolution method results support the hypothesis that the silane treatment of aluminum in this study caused an adverse effect on coupling most likely due to the method of application. This hypothesis could be proven by using lower temperatures to cure silane treated surfaces for lap shear and dissolution method samples for comparison to the current results.

From the data presented in Figure 13, it is difficult to conclude if there is substantial effect of material phase (LC or isotropic) on lap shear strength. Samples treated with PAA and PAA + BR-127 showed an increase in lap shear strength for samples cured in the LC state over samples cured in the isotropic state. Other samples showed the opposite trend. Although only these two treatment conditions showed an increase in lap shear strength for the LC cure cycle, these treatment conditions are within the group of samples that failed cohesively but were not treated with silane. As previously mentioned, it is likely that a tightly crosslinked silane network formed on the surface of the aluminum and reduced the effects of the PAA treatment. It is also possible that the silane network reduced the effects of an LC morphology within the adhesive by interfering with stress transfer at the bond line.

3.3.3 Effect of Sample Fabrication Method on Lap Shear Strength

Throughout this study, a previously described method was used to make lap shear coupons (Section 2.5). This method was a slight modification from the ASTM standard for lap shear coupon fabrication and testing. In order to compare the effect of the standard and modified methods, lap shear coupons treated with PAA and BR-127 were prepared using both fabrication methods. Two sets of samples for each fabrication method were prepared; one set cured in the LC state and the other cured in the isotropic state.

Cohesive failure occurred in the samples prepared using the ASTM standard, which is the same as the samples prepared using the modified standard. The average lap shear strengths for the ASTM standard samples were a little higher (~5-15%) than the lap shear strengths for the modified standard samples. These results are shown in Figure 14. The slight difference in lap shear strength and data scatter could be attributed to the effects of individual coupon fabrication (modified standard) as opposed to bulk coupon fabrication (ASTM standard). Individual fabrication of coupons allows for some adhesive to flow out or retract from the sides of the bondline. This effect would alter the strength of the coupon. Coupons fabricated by the ASTM standard method do not have these edge effects. Also, there is a greater chance of slight misalignment during individual coupon fabrication due to clearance gaps in the coupon jigs. This problem is avoided during bulk fabrication by cutting small coupons out of a large one to ensure parallel alignment. Despite the small differences, these results show that the modified method yields similar trends when compared to the standard method. Therefore, the modified method can be used as a quick screening tool and/or when material quantities are highly limited.

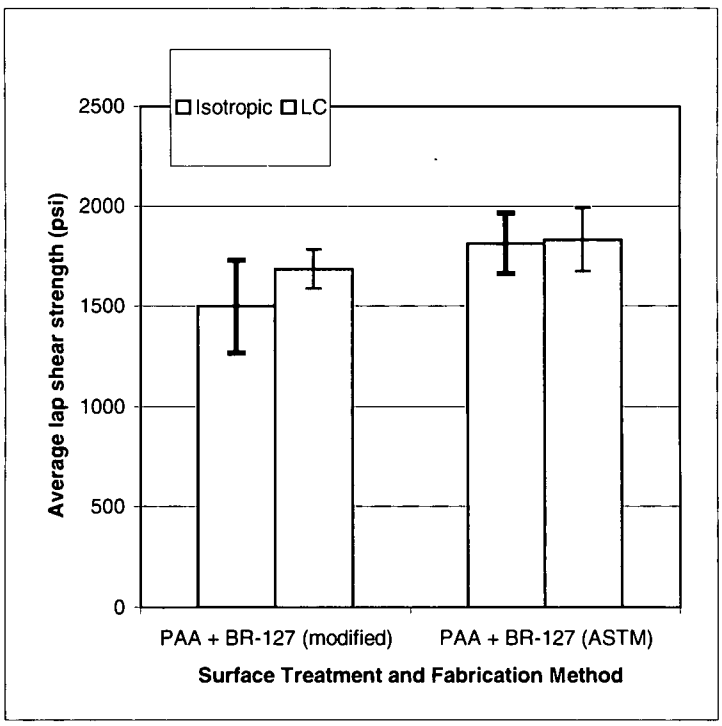

Figure 14: Comparison of fabrication method to average lap shear strength

3.3.4 Comparison of JNM-1 Lap Shear Strength to Conventional Aerospace Adhesives

JNM-1 lap shear strengths in this study are low compared to conventional film adhesives used in the aerospace industry. The highest average lap shear strength in this study was JNM-1 cured in the LC state on adherends treated with PAA and primed with BR-127 primer. When these coupons were fabricated using the ASTM method, the average lap shear strength was 1835 psi. Lap shear strengths of epoxy film adhesives made by American Cyanamid ranged from 2800 psi to 6000 psi.[2]. The comparison of lap shear strengths shows that JNM-1 does not currently exhibit the mechanical properties of conventional aerospace adhesives at room temperatures. However, JNM-1 is a highly crosslinked model compound that was expected to be brittle. JNM-1 may be expected to retain it's properties to a higher degree at high temperatures than some toughened epoxy adhesives, although that data remains to be collected. Also, other compounds similar to JNM-1 may be synthesized to include chemical features that enhance toughness, such as longer alkyl spacers. In any case, the major conclusion is that the data does not overwhelmingly support the hypothesis that the LC phase would increase the strength or toughness of the resin. However, further study is needed of JNM-1 in the aligned phase. This may lead to the desired result that the LC phase can be exploited to toughen an inherently brittle thermoset polymer.

CHAPTER IV

CONCLUSIONS

Overall analysis of the bonding process in this work shows that cohesive failure is necessary to reveal the strength of the adhesive. Adhesive failure of a bond shows that the interface strength is less than the strength within the adhesive and that the specific surface treatment or adhesive application did not promote strong interface interactions. In this study, gritblasting of aluminum adherends with or without further treatment resulted in adhesive failure in the lap shear coupons. PAA treatment of aluminum adherends with or without further treatment revealed cohesive failure during lap shear testing, and consequently, higher lap shear strengths. These results show that the use of PAA treatment on aluminum is critical to determine the cohesive strength of the bond between aluminum and JNM-1.

Whereas PAA treatment was crucial to high lap shear strengths, the application of silane in addition to PAA treatment caused a decrease in lap shear strength for samples cured in the LC phase. The decrease in lap shear strength was most likely the result of an inhibited interaction between the PAA treated surface and the JNM-1 monomer. It is likely that this inhibition is a result of the formation of a highly crosslinked silane network on the surface due to the high cure temperatures during the silane application procedure. An increase in lap shear strengths may be possible if the surface interaction were improved using lower cure temperatures during the silane application procedure [38].

Two different cure cycles were developed to cure the monomer in the isotropic and LC phase using Differential Scanning Calorimetry and polarized optical microscopy. These cure cycles were used to cure the adhesive on lap shear coupons for testing. The

lap shear results show that there is no substantial effect of either material phase on lap shear strength.

Due to the large number of samples used in this study and a limited amount of material, a modified fabrication method was used to prepare lap shear coupons in a timely manner. Lap shear strengths from coupons prepared using the modified method yielded similar trends when compared to coupons prepared using the ASTM standard method. The scatter in data observed in sample sets prepared with the modified method was attributed to edge effects and slight misalignment of the individual lap shear coupons. These effects are not as prevalent in samples prepared using the ASTM standard method.

JNM-1 lap shear strengths in this study are low compared to conventional film adhesives used in the aerospace industry. Although this adhesive does not currently possess the mechanical qualities of an aerospace adhesive, further research could help produce increased strengths. For example, further research into the effects of the silane treatment procedure may reveal an optimal silane coupling agent coverage. Use of this optimal silane coverage may improve JNM-1 lap shear strengths. Also, research into alignment of the LC phase in JNM-1 may produce a cure network with better mechanical properties than that observed with the current applications.

References

1. A.R. Meath, "Epoxy Resin Adhesives" in *Handbook of Adhesives*, ed. I. Skeist, 3rd ed., Van Nostrand Reinhold, New York (1990) 347-348.
2. R.E. Politi, "Structural Adhesives in the Aerospace Industry" in I. Skeist, in ref. 1, 713-728.
3. B.A. Dietsch, D. Klosterman, T. Tong, R. Chartoff, C. Theodore, P. Hood, "Surface Preparation of Aluminum for Adhesive Bonding of a Liquid Crystal Thermoset", Proceedings of the 46th International SAMPE Symposium and Exhibition, Long Beach, CA, May 6-10, 2001
4. R.E. Johnson, Jr. and R.H. Dettre, "Wettability and Contact Angles", *Surface and Colloid Science*, Vol. 2, ed. Egon Matijevic, Wiley and Sons, New York, 85-153 (1969).
5. J.D. Andrade, et al., "The Contact Angle and Interface Energetics" in *Surface and Interfacial Aspects of Biomedical Polymers, Vol 1*, Plenum Press, New York, 249-292 (1985).
6. E.L. Decker, et al., "Physics of Contact Angle Measurement", *Colloids and Surfaces A: Physicochem. Eng. Aspects*, **156**, 177-189 (1999).
7. J. R. Fried, *Polymer Science and Technology*, Prentice Hall, Upper Saddle River, NJ, 364-366 (1995).
8. A.V. Tobolsky, and H.F. Mark, *Polymer Science and Materials*, Wiley and Sons, New York, 123-125 (1971).
9. E.T. Samulski, "The Mesomorphic State" in *Physical Properties of Polymers*, ed. J.E. Mark, 2nd ed., American Chemical Society, Washington, D.C., 201-214 (1993).
10. J.S. Ullett, T. Benson Tolle, J.W.Schultz, R.P. Chartoff, "Thermal Expansion and Fracture Toughness Properties of Parts Made from Liquid Crystal Stereolithography Resins," *Materials and Design*, **20**, 91-97 (1999).
11. M. Giamberini, E. Amendola, C. Carfagna, "Liquid Crystalline Epoxy Thermosets", *Molecular Crystals and Liquid Crystals Science and Technology, Section A: Molecular Crystals and Liquid Crystals*, **266**, 9-22 (1995).
12. C. Carfagna, E. Amendola, M. Giamberini, "Rigid Rod Networks: Liquid Crystalline Epoxy Thermosets", *Composite Structures*, **27**, 37-43 (1994).
13. D.J. Broer, H. Finklemann, K. Kondo, *Makromol. Chem.*, **189**, 185-194 (1988).
14. H. Andersson, U.W. Gedde, A. Hult, *Polymer*, **33**(19), 4014-4018 (1992).
15. S. Jahromi, J. Lub, G.N.Mol, *Polymer*, **35**(3), 622-629 (1994).
16. W. Mormann, *Trends in Polym. Sci*, **13**(8), 255-261 (1995).
17. J.W. Schultz, R.P. Chartoff, *Polymer*, **39**(2), 319-325 (1998).

18. J.W. Schultz, R.P. Chartoff, J.S. Ullett, *J. Polym. Sci.: Part B: Polym. Phys.*, **36**(6), 1081-1089 (1998).

19. J.W. Schultz, J. Bhatt, R.P. Chartoff, R.T. Pogue, J.S. Ullett, "Polymerization and Viscoelastic Behavior of Networks from a Dual-Curing, Liquid Crystalline Monomer," *J. Polym. Sci.: Part B: Polym. Phys.*, **37**.

20. R.F. Wegman, Surface Preparation Techniques for Adhesive Bonding, Noyes Publications, Park Ridge, 1989, pp. 1-35.

21. "Standard Guide for Preparation of Aluminum Surfaces for Structural Adhesives Bonding (Phosphoric Acid Anodizing)", D3933-98, American Society for Testing Materials.

22. J.D. Venables, Journal of Materials Science, **19**, 2431-2453 (1984).

23. A.N. Gent and G.R. Hamed, "Fundamentals of Adhesion" in I. Skeist, in ref. 1, 48-51.

24. C.L. Mahoney, "Surface Preparation for Adhesive Bonding" in I. Skeist, in ref. 1, 74-80.

25. H.M. Clearfield, D.K.McNamara, and G.D. Davis, "Surface Preparation of Metals", Adhesive and Sealants, Engineered Materials Handbook, Vol.3, H.F. Brinson, Technical Chairman, ASM International, 1990.

26. Personal conversation with Jim Huff, Senior Material Technician, AFRL/MLSA, Dayton, OH, April 15, 2001.

27. A.W.Bethune, "Durability of Bonded Aluminum Structures", *SAMPE Journal*, **11**, 4-10 (1975).

28. "Standard Guide for Preparation of Metal Surfaces for Adhesives Bonding", D2651-95, American Society for Testing Materials.

29. E. Plueddemann, Silane Coupling Agents, 2nd ed., Plenum Press, New York (1991).

30. A. Popp, Effects of Morphology and Cross-Link Density on the Properties of a Dual-Curing, Liquid Crystalline Polymer, M.S. Thesis, University of Dayton, December 2000.

31. W.D. Bascom, "Primers and Coupling Agents" in H.F.Brinson, in ref 23, pp. 254-258.

32. B. Arkles, *Chemtech*, **7**, 766-778 (1977).

33. E. Fekete, B. Pukanszky, A. Toth, I. Bertoti, "Surface Modification and Characterization of Particulate Mineral Fillers", *Journal of Colloid and Interface Science*, **135**, 200-208, (1990).

34. E. Fekete, B. Pukanszky, "Surface Coverage and Its Determination: Role of Acid-Base Interactions in the Surface Treatment of Mineral Fillers", *Journal of Colloid and Interface Science*, **194**, 269-275 (1997).

35. Z. Demjén, B. Pukanszky, E. Foldes, J. Nagy, "Interaction of Silane Coupling Agents with $CaCO_3$", *Journal of Colloid and Interface Science*, **190**, 427-436 (1997).

36. J. Gulyas, S. Rosenberger, E. Foldes, B. Pukanszky, "Chemical Modification and Adhesion in Carbon Fiber/Epoxy Micro-Composites; Coupling and Surface Coverage", Institute of Chemistry, Chemical Research Center, Hungarian Acadamy of Sciences, unpublished work.

37. "Standard Test Method for Apparent Shear Strength of Single-Lap-Joint Adhesively Bonded Metal Specimens by Tension Loading (Metal-to-Metal)", D1002-01, American Society for Testing Materials.

38. N.H. Sung, A. Kaul, I. Chin, and C.S.P. Sung, *Polym. Eng. Sci.*, **22**, 637 (1982).

39. Venables, J.D., McNamara, D. K., Chen, J. M., Sun, T. M., and Hopping, R. L., *Applied Surface Science*, **3**, 88 (1979).

R00258992 7